

1st Place Solution for ICCV 2023 OmniObject3D Challenge: Sparse-View Reconstruction

Hang Du*, Yaping Xue*, Weidong Dai, Xuejun Yan, Jingjing Wang
Key Laboratory of Peace-building Big Data of Zhejiang Province

duhang.shu@foxmail.com

1. Introduction

In this report, we present the 1st place solution of team “hri test” to ICCV 2023 OmniObject3D Challenge Track-1 Sparse-View Reconstruction [1]. We ranked first in the final challenge test with a PSNR of 25.44614. The challenge aims to evaluate approaches for novel view synthesis and surface reconstruction using only a few posed images of each object. The number of input images varies from 1, 2 to 3, respectively. Such scenario is a very challenging setting for novel-view synthesis and surface reconstruction. In the following, we will provide our solution and findings in the experiment.

2. Method

In our solution, we choose NeRF-based methods as the fundamental approach for sparse-view reconstruction. Specifically, we pre-train Pixel-NeRF [10] model to learn prior knowledge across different object categories from OmniObject3D training dataset [8], and then fine-tune the model on each test sense in a short period of time. Original NeRF [5] model represents each scene as a function of colors and volume densities, optimizing the network on the dense views of every scene independently. To improve the generalization ability of NeRF models on few input images, Pixel-NeRF uses a local CNN to extract features from the input images. The overview architecture of Pixel-NeRF is shown in Figure 1. One can refer to their original paper for more details. Furthermore, we explore two additional strategies to improve the performance of the Pixel-NeRF model on sparse-view reconstruction, including depth supervision, and coarse-to-fine positional encoding.

2.1. Depth Supervision

Recently, several methods [3, 11, 7] develop depth constraints to improve the quality of surface reconstruction. Here, we use ground-truth depth maps to optimize the NeRF density function. To this end, we obtain the depth of each

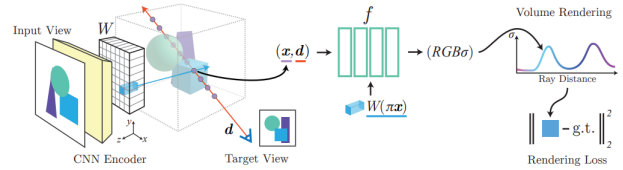


Figure 1: Overview architecture of Pixel-NeRF [10]. For a query point x along a target ray with view direction d , they extract a corresponding feature from the image feature volume W via projection and interpolation. Then, they feed the feature with spatial coordinates into the NeRF model, and predict RGB color values for neural rendering.

ray by

$$d_{\mathbf{r}} = \sum_{i=1}^N w_i t_i, \quad (1)$$

where $w_i = T_i(1 - \exp(-\sigma_i \delta_i))$, $T_i = \exp(-\sum_{j=1}^{i-1} \sigma_j \delta_j)$, $\delta_i = t_i - t_{i-1}$, σ_i is the predicted volume density from the network, and t_i is the sampled point along the ray. Then, we directly compute MSE loss between the predicted depth $d_{\mathbf{r}}$ and ground-truth depth $\hat{d}_{\mathbf{r}}$ for all camera rays \mathbf{R} of target pose \mathbf{P} as

$$\mathcal{L}_{\text{depth}} = \sum_{\mathbf{r} \in \mathbf{R}(\mathbf{P})} \|d_{\mathbf{r}} - \hat{d}_{\mathbf{r}}\|^2. \quad (2)$$

Thus, the total training supervision consists of the rendered RGB pixel value and depth for each camera ray \mathbf{r} .

2.2. Coarse-to-fine Positional Encoding

In addition, certain studies [9, 4, 6] find that high-frequency inputs are prone to the over-fitting issue in sparse-view reconstruction. To tackle this problem, they propose a similar idea of gradually activating the high-frequency components of the positional encodings during the optimization process. By doing so, they aim to prevent NeRF models from immediately overfitting to the sparse-view training images. Thus, we follow the manner of BARF [4] to assign

*These authors contributed equally to this project.

weights to the k -th frequency component of positional encoding,

$$\gamma_k(\mathbf{x}; \alpha) = w_k(\alpha) \cdot [\cos(2^k \pi \mathbf{x}), \sin(2^k \pi \mathbf{x})], \quad (3)$$

where $w_k(\alpha)$ is the weight function as

$$w_k(\alpha) = \begin{cases} 0 & \text{if } \alpha < k \\ \frac{1 - \cos((\alpha - k)\pi)}{2} & \text{if } 0 \leq \alpha - k < 1 \\ 1 & \text{if } \alpha - k \geq 1 \end{cases} \quad (4)$$

where $\alpha \in [0, L]$ is a controllable parameter proportional to the iteration of training process, and L is the number of frequency bands. As the training process, such manner will activate more higher frequency bands of the encodings.

3. Experiments

In this section, we provide more implementation details and experimental results.

3.1. Data Preparation

Following the guidelines of Track-1, we utilize OmniObject3D [8] as the initial training dataset. OmniObject3D is a large-scale 3D object dataset, and thus requires an expensive cost when trained on the whole dataset. To reduce the training consumption, we select representative categories which share the same semantics or similar shape with the 80 test scenes. By doing so, we obtain about 48 training categories from the original full dataset. The details of 48 training categories can be found in the source code. Moreover, we also construct a validation set which consists of 80 test scenes from the above 48 training categories. This validation set allows us to evaluate the performance of our model locally.

3.2. Implementation Details

We implement Pixel-NeRF from the official code [2] in the experiment. For the image encoder, we use a ResNet34 backbone pre-trained on ImageNet and all categories in OmniObject3D training dataset. Then, we optimize the model for about 1.3 million iterations on four P40 GPUs. Finally, we fine-tune the pertained model on each test scene in 5K iteration. All training hyper-parameters are given in the source code.

3.3. Results on Validation Set

Ablation of training data. We first provide the performance comparison under two training subsets in Table 1. The first line of the table corresponds to the model trained on the 10 categories with the most various scenes selected by OmniObject3D [8], while the second line represents

Table 1: Performance comparisons of two training datasets.

Method	PSNR			Chamfer Distance (CD)		
	1-view	2-view	3-view	1-view	2-view	3-view
10 Categories	19.436	24.409	24.471	0.0393	0.0349	0.0303
48 Categories	20.885	25.133	25.327	0.0388	0.0321	0.0282

Table 2: Ablation of additional model components.

Method	PSNR			Chamfer Distance (CD)		
	1-view	2-view	3-view	1-view	2-view	3-view
baseline	19.436	24.409	24.471	0.0393	0.0349	0.0303
+ DS	19.188	24.459	24.958	0.0368	0.0318	0.0280
+ C2FPE	18.610	24.773	24.692	0.0398	0.0349	0.0304
+ FT encoder	19.757	24.490	24.687	0.0390	0.0360	0.0307
Full model	19.304	24.877	25.119	0.0384	0.0312	0.0275

Table 3: Study of different test-time optimization strategies.

Method	PSNR			Chamfer Distance (CD)		
	1-view	2-view	3-view	1-view	2-view	3-view
w/o fine-tuning	21.645	23.362	24.757	0.0394	0.0339	0.0293
freeze encoder	25.081	26.249	28.603	0.0344	0.0264	0.0210
freeze rendering	23.279	25.829	28.937	0.0387	0.0277	0.0202
Full fine-tuning	25.116	25.881	28.679	0.0353	0.0279	0.0207

training on the 48 representative categories mentioned earlier. From the results, we can observe that our representative categories provide abundant information for learning the object priors, and thus obtain better novel-view results.

Ablation of model components. We also conduct ablation study on each model component. As shown in Table 2, the “DS” denotes the extra depth supervision, the “C2FPE” represents the coarse-to-fine positional encoding method, and “FT encoder” is to fine-tune the image encoder on all categories in OmniObject3D training dataset. The “Full model” refers to the model that incorporates all the model components. Moreover, the depth supervision is effective to predict more accurate depth and improve the density field modeling, resulting in a better fidelity of surface reconstruction.

Study of test-time optimization. Furthermore, we try different object-level fine-tuning strategies. Specifically, we freeze the encoder or rendering module during the test-time optimization. Note that the model is only evaluated on the half of validation set, due to the limited computation resources. From the results in Table 3, we can conclude that object-level fine-tuning is crucial in improving the quality of sparse-view reconstruction, particularly for unseen scenes. This optimization step helps the model adapt to the specific characteristics of each test scene, resulting in better reconstruction results.

Table 4: Performance comparisons on challenge test.

Method	PSNR	CD
w/o fine-tuning	23.32744	0.03268
w fine-tuning	25.44614	0.02794



Figure 2: Qualitative comparisons on challenge test. The first line of each object is generated by the pre-trained model, and the second line is generated by each object-level fine-tuned model.

3.4. Results on Challenge Test

Here, we report more results on the challenge test. As mentioned before, we pre-train the Pixel-NeRF model on the representative 48 categories, and then fine-tune the model on each test scene. The results are presented in Table 4. Moreover, as shown in Figure 2, we can clearly observe improved results achieved by the fine-tuning process.

4. Conclusion

In this report, we introduce the details of our solution to ICCV 2023 OmniObject3D Challenge Track-1. We utilize Pixel-NeRF as the basic model, and apply depth supervision as well as coarse-to-fine positional encoding. The experiments demonstrate the effectiveness of our approach in improving sparse-view reconstruction quality. We ranked first in the final test with a PSNR of 25.44614.

References

- [1] <https://omniobject3d.github.io/challenge.html>.
- [2] <https://github.com/sxyu/pixel-nerf>.
- [3] Kangle Deng, Andrew Liu, Jun-Yan Zhu, and Deva Ramanan. Depth-supervised nerf: Fewer views and faster training for free. In *Proceedings of the IEEE/CVF Conference on Computer Vision and Pattern Recognition*, pages 12882–12891, 2022.
- [4] Chen-Hsuan Lin, Wei-Chiu Ma, Antonio Torralba, and Simon Lucey. Barf: Bundle-adjusting neural radiance fields. In *Proceedings of the IEEE/CVF International Conference on Computer Vision*, pages 5741–5751, 2021.
- [5] Ben Mildenhall, Pratul P Srinivasan, Matthew Tancik, Jonathan T Barron, Ravi Ramamoorthi, and Ren Ng. Nerf: Representing scenes as neural radiance fields for view synthesis. In *European Conference on Computer Vision*, pages 405–421. Springer, 2020.
- [6] Prune Truong, Marie-Julie Rakotosaona, Fabian Manhardt, and Federico Tombari. Sparf: Neural radiance fields from sparse and noisy poses. *2023 IEEE/CVF Conference on Computer Vision and Pattern Recognition (CVPR)*, pages 4190–4200, 2022.
- [7] Guangcong Wang, Zhaoxi Chen, Chen Change Loy, and Ziwei Liu. Sparsenerf: Distilling depth ranking for few-shot novel view synthesis. *arXiv preprint arXiv:2303.16196*, 2023.
- [8] Tong Wu, Jiarui Zhang, Xiao Fu, Yuxin Wang, Jiawei Ren, Liang Pan, Wayne Wu, Lei Yang, Jiaqi Wang, Chen Qian, et al. Omniobject3d: Large-vocabulary 3d object dataset for realistic perception, reconstruction and generation. In *Proceedings of the IEEE/CVF Conference on Computer Vision and Pattern Recognition*, pages 803–814, 2023.
- [9] Jiawei Yang, Marco Pavone, and Yue Wang. Freenerf: Improving few-shot neural rendering with free frequency regularization. In *Proceedings of the IEEE/CVF Conference on Computer Vision and Pattern Recognition*, pages 8254–8263, 2023.

- [10] Alex Yu, Vickie Ye, Matthew Tancik, and Angjoo Kanazawa. pixelnerf: Neural radiance fields from one or few images. In *Proceedings of the IEEE/CVF Conference on Computer Vision and Pattern Recognition*, pages 4578–4587, 2021.
- [11] Zehao Yu, Songyou Peng, Michael Niemeyer, Torsten Sattler, and Andreas Geiger. Monosdf: Exploring monocular geometric cues for neural implicit surface reconstruction. *Advances in neural information processing systems*, 35:25018–25032, 2022.